INFLUENCE OF Al_2O_3-ZrO_2 AGEING ON ZrO_2 PHASE TRANSFORMATION AND OSTEOBLAST CELL RESPONSE

M. P. Albano[a], H. L. Calambás Pulgarin[a], L. B. Garrido[a] , P. Tambasco de Oliveira[b], A. L. Rosa[b]

[a] Centro de Tecnología de Recursos Minerales y Cerámica (CETMIC), CCT-La Plata CONICET, CICPBA, C.C. 49 (B1897ZCA) M. B. Gonnet, Provincia de Buenos Aires, ARGENTINA.
[b] School of Dentistry of Ribeirão Preto, University of São Paulo (FORP-USP).
E-mail: palbano@cetmic.unlp.edu.ar

ABSTRACT

Two commercial 3 mol% yttria stabilized zirconia, with 0.3 wt% Al_2O_3 (YZA) and without Al_2O_3 (YZ), were used to produce alumina-zirconia slip cast composites. The influence of the ZrO_2 content and the ZrO_2 grain size on the ageing behaviour of the different Al_2O_3-ZrO_2 composites were investigated. In addition, the biocompatibility and osteogenic differentiation of Al_2O_3-ZrO_2 surfaces were evaluated before and after ageing using osteoblast cell culture. The ageing susceptibility of the composites significantly increased with increasing the ZrO_2 content over 22 vol%. For 50 vol% ZrO_2, the greater grain size of YZ composites with respect to those YZA enhanced the ageing degradation. The mineralization of cells grown on 50 vol% YZ was significantly higher than that on 50 vol% YZA. The ageing process on 50 vol% YZA stimulated early cell proliferation and promoted differentiation, whereas the production of mineralized matrix markedly reduced on the aged 50 vol% YZ.

Key-words: Al_2O_3-ZrO_2; ageing behavior; cell proliferation; matrix mineralization.

INTRODUCTION

Extensive research has focused on the development of the so-called zirconia-toughened alumina composites (ZTA), materials with enhanced flexural strength, fracture toughness, and fatigue resistance mainly as a consequence of the stress-

induced zirconia phase transformation (1, 2). However, since these ceramics contain zirconia, they are likely to undergo ageing i.e. the low temperature degradation (LTD) of zirconia. When 3 mol% yttria stabilized zirconia (Y-TZP) is exposed to an aqueous environment at 100-300 °C over long periods, Y-TZP surface transforms spontaneously into the monoclinic structure via a stress-corrosion-type mechanism (3). This transformation is accompanied by a 4 vol% increase and 16% shear, leading to microcracking, surface roughening, and eventually grain pullout. The process continuously proceeds from the surface to the bulk of Y-TZP, resulting in a volumetric expansion followed by failure (3).

Recently (2), we have studied the sintering behaviour and microstructure development of different Al_2O_3-ZrO_2 composites. The microstructural characterization revealed that the composites obtained using two Y-TZP powders, with 0.25 wt% Al_2O_3 (YZA) and without Al_2O_3 (YZ) had different zirconia mean grain sizes (2). The ageing susceptibility of Y-TZP is strongly dependent on its grain size (4). In this work, Al_2O_3- ZrO_2 composites with different zirconia contents were produced by slip casting from such commercial YZ and YZA powders and therefore, the influence of the ZrO_2 content and the ZrO_2 grain size on the ageing behaviour of both ceramics were investigated. Also, it is believed that the zirconia content and the different physicochemical characteristics of YZ and YZA powders may affect the Al_2O_3-ZrO_2 biocompatibility. Thus, the t -m zirconia transformation during ageing can induce cell proliferation due to the creation of a roughness surface layer of monoclinic phase on the Al_2O_3-ZrO_2 ceramics. In addition, the biocompatibility and osteogenic differentiation of the different Al_2O_3- ZrO_2 surfaces were evaluated before and after ageing using bone marrow-derived osteoblast cell culture.

EXPERIMENTAL PROCEDURE

Ceramic preparation and characterization

Two commercially available Y-TZP with 0.25 wt% Al_2O_3 (YZA) and without Al_2O_3 (YZ) (Saint-Gobain ZirPro, China) were used in this study. The average particle size of YZA and YZ was 0.21 μm and 0.4 μm, respectively.

Al_2O_3-ZrO_2 compositions with different YZA and YZ contents, 10.5, 22 and 50 vol%, were used to prepare the composites. Aqueous 48 vol% Al_2O_3-ZrO_2 suspensions with the different compositions and the optimum ammonium polyacrylate (NH4PA)

concentration (Duramax D 3500, Rohm & Haas) were prepared by ultrasound; the pH was adjusted at 9 with ammonia (25 %). Slips were cast in plaster molds into rectangular bars (12 x 10 x 9 mm). The samples were dried at 100 °C and sintered at 1600 °C for 2 h (heating rate 5 °C/min).

The zirconia grain sizes were measured using SEM micrographs (JEOL, JSM-6360) of polished and thermally etched surfaces. The grain size values were the average of about a hundred measurements.

The biological assays were carried out using Al_2O_3-ZrO_2 disks, 12 mm in diameter and 3 mm thickness, produced by slip casting and sintered at 1600 °C for 2 h.

Al_2O_3-ZrO_2 ageing

The ageing degradation experiments were carried out in an autoclave at 134 °C under 2-bars pressure at increasing time up to 24 h (1h in autoclave is theoretically equivalent to 3-4 years in vivo (5).

Phase identification was done by X-ray diffraction (XRD) analysis (Philips 3020 equipment) using Cu-Kα radiation with Ni filter at 40 kV–20 mA. The influence of the ageing on the ZrO2 t-m transformation was quantitatively evaluated by XRD. The volume fractions of monoclinic and tetragonal ZrO2 on the surfaces of the composites were calculated using the Rietveld method as described in (2). Sintered samples before and after ageing were cut and polished for microstructural observation by SEM.

The changes in surface topography after ageing were examined by AFM (Multimode-Nanoscope V, Veeco, Santa Barbara, CA) in contact mode. The used silicon nitride probes had a nominal spring constant of 0.06 N/m and a nominal tip radius of curvature of 10 nm.

Biological assays

1. Cell isolation and culture of bone marrow-derived osteoblast cells

The cells were obtained from the femora of bone marrow of young adult male rats (Rattus norvegicus, Wistar) weighing 120 g as described previously (6), under the guidance of the Ethics Committee on Animal Use of the University of São Paulo at Ribeirão Preto (Protocol Number 2015.1.1136.58.1). The released cells were collected in a 75 cm^2 culture flask (Corning Incorporated, NY) containing 10 mL of osteogenic medium (OM) composed by MEM supplemented with 10% fetal bovine

serum (Invitrogen) and 500 µg/mL gentamycin (Invitrogen) supplemented with 5 µg/mL ascorbic acid, 7 mM glycerophosphate (Sigma-Aldrich, St. Louis, MO), and 10^{-7} M dexamethasone (Sigma-Aldrich). The flasks were incubated at a 37 ºC in a humidified atmosphere of 5% CO_2 and 95% air. The medium was changed every 3 days. After 7-10 days, first passage cells were counted and seeded in 24-well culture plates (Corning) containing the disks immersed in 1.8 mL of OM, at a plating density of $2x10^4$ cells/well. Cells seeded in wells without disks were used as controls. During the culture period, cells were incubated at 37 ºC in a humidified atmosphere of 5% CO_2 and 95% air, for up to 17 days.

2. Cell morphology

At day 1 of culture, bone marrow-derived osteoblast cell morphology was evaluated by direct fluorescence to detect the actin cytoskeleton and cell nuclei (7). Briefly, cells were fixed for 10 min at RT using 4% paraformaldehyde in 0.1 M sodium phosphate buffer (PB), pH 7.2. After being washed in PB, cultures were permeabilized with 0.5% Triton X-100 in PB for 10 min and processed for fluorescence labeling. Alexa fluor 594 (red fluorescence)-conjugated phalloidin (1:200, Molecular Probes, Eugene, OR) was used to label the actin cytoskeleton. Before mounting for microscope observation, samples were washed with deionized water (dH_20), and the cell nuclei were stained with 300 nM 40,6-diamidino-2-phenylindole, dihydrochloride (DAPI, Molecular Probes) for 5 min. The disks were placed face up on glass slides, covered with 12-mm round glass coverslips (Fisher Scientific, Grand Island, NY) and mounted with an antifade kit (Vectashield, Vector Laboratories, Burlingame, CA). The samples were then examined under epifluorescence, using a Zeiss AxioImager M2 microscope (Carl Zeiss, Oberkochen, Germany) outfitted with an AxioCam MRm digital camera (Carl Zeiss).

3. Cell viability

Cell viability was evaluated by 3-[4,5-dimethylthiazol-2-yl]-2,5-diphenyl tetrazolium bromide (MTT, Sigma-Aldrich) assay, which measures the mitochondrial activity of viable cells (8). At day 7 of culture, bone marrow-derived osteoblast cells were incubated with 10% MTT (5 mg/mL) in culture medium at 37 °C for 4 h. The medium was then aspirated from the well, and 1 mL acid isopropanol (0.04 N HCl in isopropanol) was added to each well. The plates were then stirred on a plate shaker

for 5 min, and 150 µL of this solution was transferred to a 96-well format using opaque-walled transparent-bottomed plates (Corning). The optical density was read at 570-650 nm on the plate reader (µQuanti, BioTek Instruments Inc., Winooski, VT), and data were expressed as absorbance.

4. Extracellular matrix mineralization

At day 17 of bone marrow-derived osteoblast cells were fixed in 10% formalin for 2 h at RT, dehydrated and stained with 2% Alizarin Red S (Sigma-Aldrich), pH 4.2, for 10 min. The images were acquired using a high-resolution camera (Canon EOS Digital Rebel, 6.3 MP) and processed using Adobe Photoshop CS5.1 software (Adobe Systems). The calcium content was detected using a colorimetric method (9). Briefly, 280 µL of 10% acetic acid were added to each well, and the plate was incubated at RT for 30 min under shaking. This solution was heated to 85 ºC for 10 min, and transferred to ice for 5 min. The slurry was centrifuged at 20,000 g for 15 min, and 100 µL of the supernatant was mixed with 40 µL of 10% ammonium hydroxide. This solution was spectrophotometrically read at 405 nm in the plate reader µQuant (Biotek), and the data were expressed as absorbance.

5. Statistical analysis

The data were expressed as means ± standard deviations and analyzed by one-way ANOVA. Post-test was carried out by Tukey-b test when appropriate. For all comparisons, the level of significance (*p*) was set at 0.05.

RESULTS

Ageing behavior

The rate at which the tetragonal phase is transformed to monoclinic phase is an indication of the ageing sensitivity of the Al_2O_3-ZrO_2 ceramics (4). Figure 1 shows that the monoclinic ZrO_2 content of the composites with 10.5 and 22 vol% ZrO_2 slightly changed with prolonged ageing time up to 24 h and remained below 8-9 vol% and 4-5 vol% for 22 and 10.5 vol% ZrO_2, respectively. The ageing susceptibility of Al_2O_3-ZrO_2 composites significantly increased with increasing the ZrO_2 content from 22 to 50 vol%. The curves of the composites with 50 vol% ZrO_2 quickly rose during the first 6 h of ageing, indicating that a nucleation process with constant rate occurred up to 6 h. For longer ageing time (> 6 h) the lower slope observed was

related with a reduction in the nucleation rate as the surface approached to its saturation level (i.e., when the surface is completely covered by the monoclinic nucleus) (10); in this last period, a monoclinic content of 37 and 44 vol% was reached for 50 vol% YZA and 50 vol% YZ, respectively, after 24 h of ageing. For each ageing time, the amount of transformed monoclinic zirconia on the surface of 50 vol% YZ was greater than that of 50 vol% YZA.

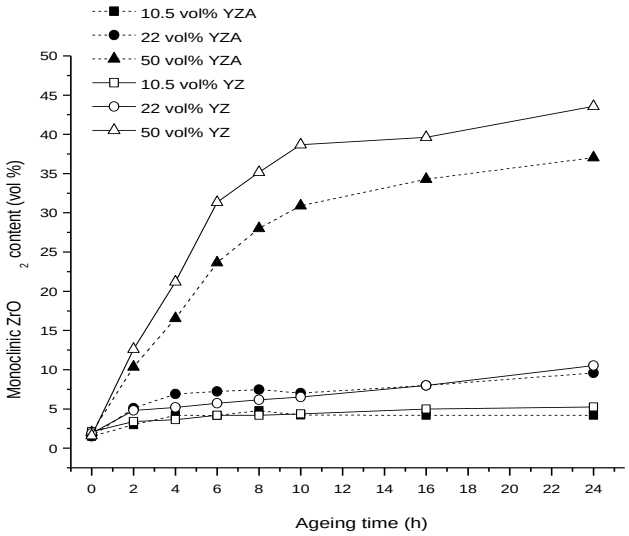

Figure 1: Monoclinic zirconia content as a function of the ageing time for the different composites.

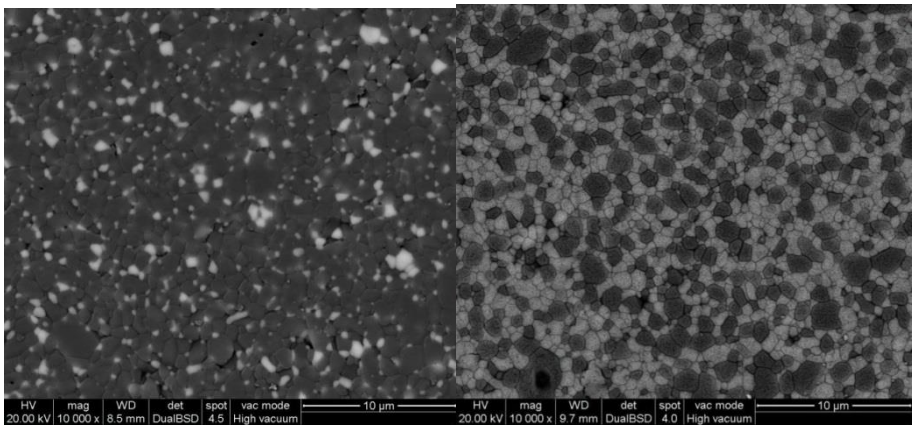

Figure 2: SEM micrographs of Al_2O_3-ZrO_2 composites with different ZrO_2 contents: (A) 10.5 vol%, (B) 50 vol%. Bright grains (ZrO_2), dark grains (Al_2O_3).

Figure 2A shows that for low ZrO_2 content (10.5 vol%), the majority of the ZrO_2 grains were isolated in the matrix, the Al_2O_3 matrix retarded progression of the

transformation by reducing the contact area between zirconia grains. Thus, propagation of the transformation from one ZrO_2 grain to another was not possible. An increase in the ZrO_2 content to 50 vol% increased the contacts between ZrO_2 grains (Figure 2B) approaching each other and promoting the propagation of the transformation. The transformation of a ZrO_2 grain triggered the transformation of a neighbour ZrO_2 grain; consequently the increase in the number of neighbouring ZrO_2 grains in 50 vol% ZrO2 allowed the transmission of the transformation shear strain. In the composites with 50 vol% ZrO_2, the reduced matrix elastic modulus (2) enhanced the nucleation of monoclinic phase, and the increase in the ZrO_2 grains contacts allowed the propagation of the transformation.

Figure 3 shows the m- ZrO_2 content after 2-10 h of ageing as a function of the ZrO_2 mean grain diameter in the different composites. The monoclinic phase content of the YZA composites with mean grain size of 0.65 and 0.70 µm (i.e. with 10.5 and 22 vol% ZrO_2, respectively) and those of YZ ceramics with mean grain size of 0.72 and 0.77 µm corresponding to 10.5 and 22 vol% ZrO_2 respectively, slightly changed with prolonged ageing time up to 10 h. Although the average grain size of 10.5 vol% and 22 vol% YZA were lower than those of YZ, there was no marked difference in ageing behavior between these composites. Thus, for ZrO_2 content ≤ 22 vol%, the grain size did not influence the transformability of t- ZrO_2 under ageing conditions.

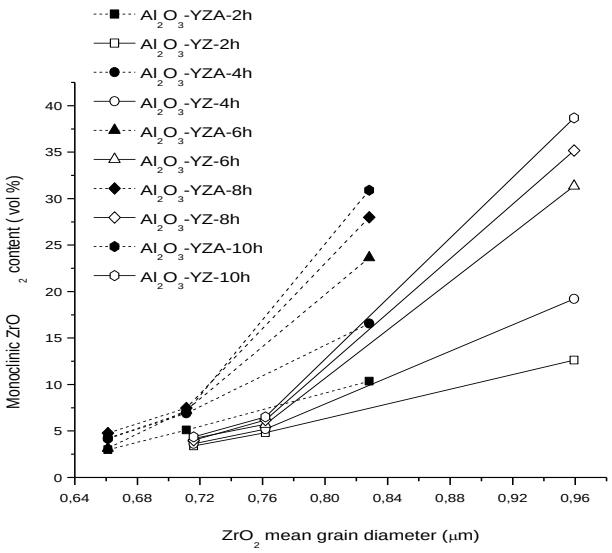

Figure 3: Monoclinic ZrO_2 content as a function of the ZrO_2 mean grain diameter in the different composites.

The ageing susceptibility of the composites significantly increased with increasing the ZrO_2 content over 22 vol% (Figure 1), which could be attributed to the decrease in the matrix elastic modulus and the coalescence of the ZrO_2 grains. We have previously found (10) that the t-m phase transformation of YZ was similar to that of YZA, thus the transformation was not improved by Al_2O_3 doping. The tetragonal phase became easier to transform with increasing their size from 0.83 µm for 50 vol% YZA to 0.96 µm for 50 vol% YZ (Figure 3). In this work, there was a clear indication that the ZrO_2 grain size was the main factor affecting the transformability of t-ZrO_2 in the composites with 50 vol% ZrO_2. For each ageing time, the greater grain size of 50 vol% YZ with respect to 50 vol% YZA enhanced the ageing degradation.

3.2. Biological studies

The osteoblast cell response to the different composites was assessed in terms of cell morphology, viability and extracellular matrix mineralization at key time points, on days 1, 7 and 21 of culture, respectively. Figure 4 shows the epifluorescence of cell cultures grown on Al_2O_3-YZ and Al_2O_3-YZA discs at day 1 of culture. No major differences in terms of cell morphology were detectable among the composites. Overall, the cells adhered to and spread on the various substrates, exhibiting polygonal shapes and establishing cell-cell contact in some regions (Figure 4).

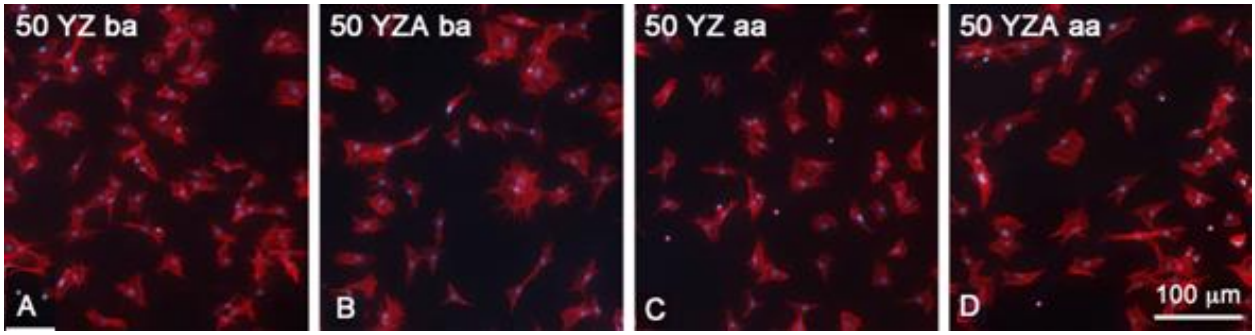

Figure 4: Epifluorescence of bone marrow-derived osteoblast cell cultures grown on Al_2O_3-YZ (A, C) and Al_2O_3-YZA (B, D) disks with 50 vol% ZrO_2 before ageing (ba) and after 2 h of ageing (aa) at day 1 of culture. Red and blue fluorescence indicate actin cytoskeleton and cell nuclei, respectively. Scale bar = 100 µm.

Figure 5 shows that at day 7 of culture, despite some variations in the MTT values, there was statistical significant difference only for the comparison between 10.5 vol% YZA ba and 10.5 vol% YZ ba composites.

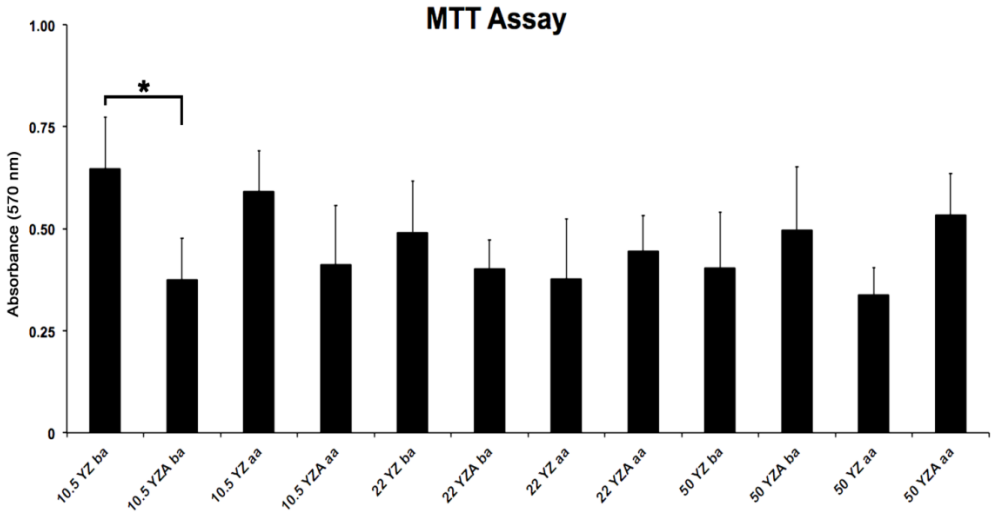

Figure 5: MTT assay of bone marrow-derived osteoblast cell culture grown on Al_2O_3-YZ and Al_2O_3-YZA disks with different ZrO_2 contents before ageing (ba) and after 2 h of ageing (aa) at day 7 of culture. The asterisk indicates statistically significant difference ($p < 0.05$).

Figure 6 shows the extracellular matrix mineralization (Ca content) of bone marrow-derived osteoblast cell culture grown on the different composites. Except for the higher mineralization of the osteoblast cells grown on 50 vol% YZ ba compared with the ones grown on 50 vol% YZA ba, there were no significant differences among groups in terms of osteogenic differentiation.

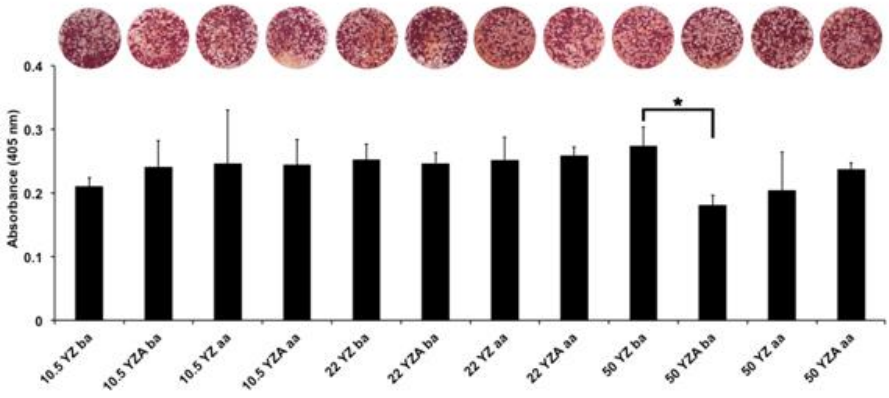

Figure 6: Extracellular matrix mineralization (Ca content) of bone marrow-derived osteoblast cell culture grown on Al_2O_3-YZ and Al_2O_3-YZA disks with different ZrO_2 contents before ageing (ba) and after 2 h of ageing (aa). The asterisk indicates statistically significant difference ($p < 0.05$).

The presence of higher amounts of Zr-OH functional groups on the YZ surface with respect to YZA could positively affect osteoblast cell functions, as demonstrated elsewhere (12). Besides, the isoelectric point (IEP) of YZA (pH_{IEP}= 8.9 (2)) was higher than that of Al_2O_3 (pH_{IEP}= 8 (2)) and YZ (pH_{IEP}= 7 (2)), therefore, the substitution of either 50 vol% Al_2O_3 or 50 vol% YZ by 50 vol% YZA resulted in a markedly decreased in the negative surface charge of 50 vol% YZA surface in the culture medium. Both the decrease in the negative surface charge and the lesser amount of Zr-OH functional groups on 50 vol% YZA ba reduced the osteogenic potential of the osteoblast cell cultures. For Al_2O_3-YZA composites before ageing, a tendency toward a decrease in the mineralization of osteoblast cells was found with increasing the YZA content from 22 to 50 vol%, which was probably due to the decrease in the negative surface charge of 50 vol% YZA surface in the culture medium.

The effect of ageing (2 h) on the osteogenic differentiation of the various Al_2O_3-ZrO_2 surfaces of ageing, given in Figure 6, indicated that there were no significant differences in the osteogenic differentiation after ageing on the composites with 10.5 and 22 vol% ZrO_2. The ageing process tended to rescue the osteogenic potential of bone marrow-derived osteoblast cells grown on 50 vol% YZA while inhibiting the one on 50 vol% YZ. The higher t-m transformation on 50 vol% YZ compared to 50 vol% YZA (Figure 1) appeared to be not favorable for the osteogenic differentiation.

The average roughness of the surface was calculated from AFM analysis, the value for 50 vol% YZA increased from 70 to 88.3 after 2 h of ageing, whereas that of 50 vol% YZ increased from 68.3 to 98.4. For 50 vol% YZ, a larger increase in surface roughness was observed, in accordance with the more pronounced t-m transformation (Figure 1). It is generally accepted that the material surface roughness at the micron and nanoscale enhances bone matrix production at the material/tissue interface *in vitro* and *in vivo* (13). The lesser surface roughness of 50 vol% YZA aa compared with 50 vol% YZ aa was found to be favorable for the progression and extracellular matrix mineralization of the bone marrow-derived osteoblast cell cultures; on the contrary, the high level of roughness of 50 vol% YZ aa appeared to be not favorable (Figure 6). There seemed to be a narrow surface roughness range between improvement and reduction of the osteogenic potential of bone marrow-derived osteoblast cells.

CONCLUSIONS

The influence of the ZrO_2 content and ZrO_2 grain size on the ageing behaviour of two different Al_2O_3- ZrO_2 composites was studied. In addition, the biocompatibility and osteogenic differentiation of the different Al_2O_3-ZrO_2 surfaces were evaluated before and after ageing using osteoblast cell cultures. When the volume fraction of ZrO_2 was kept under 22 vol%, the ageing susceptibility was reduced independently from the ZrO_2 grain size. The ZrO_2 ageing degradation significantly increased with increasing the ZrO_2 content from 22 to 50 vol%; the greater grain size of 50 vol% YZ with respect to 50 vol% YZA enhanced the ageing degradation. Overall, no significant differences among the composites before ageing were observed in terms of osteogenic differentiation, except for the higher mineralization of bone marrow-derived osteoblast cells grown on 50 vol% YZ ba compared with 50 vol% YZA ba. The ageing process tended to rescue the osteogenic potential of these cells grown on 50 vol% YZA while inhibiting the one on 50 vol% YZ

ACKNOWLEDGEMENTS

This work was financially supported by CONICET (2012/Res. D. No ^{0} 2544) and FAPESP 2012/50949-4.

REFERENCES

(1) OLHERO, S.; GANESH, I.; TORRES, P.; ALVES, F.; FERREIRA, J.M.F. Aqueous colloidal processing of ZTA composites, J. Am. Ceram. Soc. v.92,n.1, p.9-16, 2009.
(2) CALAMBÁS PULGARIN, H.L.; ALBANO, M.P. Three different alumina–zirconia composites: Sintering, microstructure and mechanical properties, Mat. Sci. Eng. A v. 639, p.136-144, 2015.
(3) KOSMAC, T.; KOLJAN, A. Ageing of dental zirconia ceramics, J. Eur. Ceram. Soc. v.32, n.11, p. 2613-2622, 2012.
(4) HALLMANN, L.; ULMER, P.; REUSSER, E.; LOUVEL, M.; HAMMERLE, C.H.F. Effect of dopants and sintering temperature on microstructure and low temperature degradation of dental Y-TZP-zirconia, J. Eur. Ceram. Soc. v. 32, n.16, p. 4091-4104, 2012.

(5) CHEVALIER, J.; DEVILLE, S.; MUNCH, E.; JULLIAN, R.; LAIR, F. Critical effect of cubic phase on aging in 3 mol% yttria-stabilized zirconia ceramics for hip replacement prosthesis, Biomaterials v. 25,n.24, p. 5539–5545, 2004.

(6) MANIATOPOULOS, C.; SODEK, J.; MELCHER, A.H. Bone formation *in vitro* by stromal cells obtained from bone marrow of young adult rats, Cell Tissue Res. v. 254, n.2, p. 317-330, 1988.

(7)SCHWARTZ, H.O.; NOVAES, JR. A.B.; DE CASTRO, L.M.S.; ROSA, A.L.; DE OLIVEIRA, P.T. *In vitro* osteogenesis on a microstructured titanium surface with additional submicron-scale topography, Clin. Oral Implants Res. v. 18, n.3, p.333-344, 2007.

(8) MOSMANN, T. Rapid colorimetric assay for cellular growth and survival: Application to proliferation and cytotoxicity assays, J. Immunol. Methods v. 65,n. 1-2, p. 55-63, 1983.

(9) GREGORY, C.A.; GUNN, W.G.; PEISTER, A.; PROCKO, P D.J. An Alizarin red-based assay of mineralization by adherent cells in culture: comparison with cetylpyridinium chloride extraction, Anal. Biochem. v. 329,n.1, p.77-84, 2004.

(10) BRUNI, Y.L.; GARRIDO, L.B.; ALBANO, M.P.; TEIXEIRA, L.N.; ROSA, A.L.; DE OLIVEIRA, P.T. Effects of surface treatments on Y-TZP phase stability, microstructure and osteoblast cell response, Ceram. Int. v. 41, n.10, p.14212-14222, 2015.

(11) PECHARROMAN, C.; BARTOLOME, J. F; REQUENA, J.; MOYA, J. S.; DEVILLE, S.; CHEVALIER, J.; FANTOZZI, G.; TORRECILLAS, R. Percolative mechanism of aging in zirconia-containing ceramics for medical applications, Adv. Mater. v.15, n.6, p.507-511,2003.

(12) ZHANG, S.; SUN, J.; XU, Y.; QIAN, S.; WANG, B.; LIU, F.; LIU, X. Adhesion, proliferation and differentiation of osteoblasts on zirconia films prepared by cathodic arc deposition, Biomed. Mater. Eng. v. 23, n.5, p.373-385, 2013.

(13) GITTENS, R.A.; OLIVARES-NAVARRETE, R.; CHENG, A.; ANDERSON, D.M.; McLACHLAN, T.; STEPHAN, I.; GEIS-GERSTORFER, J.; SANDHSGE, K.H.; FEDOROV, A.G.; RUPP, F.; BOYAN, B.D.; TANNENBAUM, R.; SCHWARTZ, Z. The roles of titanium surface micro/nanotopography and wettability on the differential response of human osteoblast lineage cells, Acta Biomater. v. 9, n.4, p. 6268-6277, 2013.